ELSEVIER

Journal of South American Earth Sciences 18 (2004) 11–25

Journal of
South American
Earth Sciences

www.elsevier.com/locate/jsames

The Paleocene travertine system of the Itaboraí basin, Southeastern Brazil

L.G. Sant'Anna[a,b,*], C. Riccomini[a,c], B.H. Rodrigues-Francisco[d], A.N. Sial[c,e], M.D. Carvalho[f], C.A.V. Moura[g]

[a]*Department of Sedimentary and Environmental Geology, Institute of Geosciences, University of São Paulo, Rua do Lago 562, 05508-080 São Paulo, SP, Brazil*
[b]*São Paulo State Research Foundation–FAPESP, Brazil*
[c]*National Council for Scientific and Technological Development–CNPq, Brazil*
[d]*Department of Geology and Paleontology, Museu Nacional/UFRJ, Quinta da Boa Vista, São Cristóvão, 20940-040 Rio de Janeiro, RJ, Brazil*
[e]*NEG-LABISE, Institute of Geosciences, Federal University of Pernambuco, CP 7852, 50732-970 Recife, PE, Brazil*
[f]*Petrobrás Research Center, Ilha do Fundão, Cidade Universitária, Q.7, 21949-900 Rio de Janeiro, RJ, Brazil*
[g]*Pará-Iso, Centre of Geosciences, Federal University of Pará, Rua Augusto Corrêa 1, 66075-110 Belém, PA, Brazil*

Received 1 November 2003; accepted 1 August 2004

Abstract

The record of pre-Quaternary travertines is restricted to relatively few publications in the geological literature. In this paper, the authors present a petrographic and geochemical study of Paleocene travertines partly exposed in the Itaboraí basin, a small half-graben of southeastern Brazil. Travertine lithofacies were defined mainly from borehole samples, and these data were integrated with available field information. The most representative lithofacies of the travertine system are crystalline crusts that developed around springs at the surface and close to the fault. Other lithofacies, such as pisoid, micritic, and lithoclast travertines and tufas, were deposited distally from the springs. Mn and Fe carried to the surface by rising waters were incorporated in CL-zoned fibrous calcite and precipitated as iron-bearing minerals, respectively. Both goethite in the crystalline crusts and pyrite in the micritic travertine probably formed under biotic mediation. The evolution of this travertine system was related to Cenozoic reactivation of a shear zone in the Precambrian basement at the southern border of the basin. $^{87}Sr/^{86}Sr$ ratios indicate that groundwaters interacted with subsurface Precambrian marbles and gneisses before reaching the surface. $\delta^{13}C$ and $\delta^{18}O$ data suggest that several factors influenced carbonate precipitation in distal settings and that crystalline crusts formed from waters that changed in composition in the spring outlets and/or downflow within the travertine system.

Keywords: Brazil; Calcite; Itaboraí basin; Paleocene; Strontium; Travertine

1. Introduction

Travertines, generally understood as limestones deposited from Ca-bicarbonate waters in hydrothermal springs (e.g. Renaut and Jones, 2000) have been described throughout the world. The main travertine deposits are of Quaternary age, such as those from Italy (Chafetz and Folk, 1984; Pentecost and Tortora, 1989; Guo and Riding, 1998), France (Pentecost, 1991, 1995), Germany (Koban and Schweigert, 1993), Turkey (Altunel and Hancock, 1993, 1994), and the United States (Waring, 1965; Pentecost, 1990; Fouke et al., 2000). They are commonly associated with calcareous tufa.

The term travertine also is commonly used in a broader sense to refer to all non-marine limestones formed under climatic controls in streams, lakes, springs, and caves (e.g. Sanders and Friedman, 1967; Viles and Goudie, 1990; Pentecost and Viles, 1994). In this paper, we define travertines as hydrothermal carbonate deposits formed by physical–chemical and microbial processes and lacking in situ macrophyte and animal remains; tufa refer to limestones precipitated in cool or near-ambient temperature

* Corresponding author. Address: Department of Sedimentary and Environmental Geology, Institute of Geosciences, University of São Paulo, Rua do Lago 562, 05508-080 São Paulo, SP, Brazil. Tel.: +55 11 3091 2867; fax: +55 11 3091 4207.
E-mail address: lsantann@hotmail.com (L.G. Sant'Anna).

0895-9811/$ - see front matter © 2004 Elsevier Ltd. All rights reserved.
doi:10.1016/j.jsames.2004.08.005

water and characterized by high micro- and macrophyte, bacteria, and invertebrate content (Ford and Pedley, 1996).

Well-preserved or still forming Quaternary travertines and tufas have been studied with regard to their depositional settings and geochemistry, as well as the processes and factors that control mineral precipitation (e.g. Fouke et al., 2000). Some pre-Quaternary travertines and tufas also have been described on the basis of comparisons with lithofacies and textures of similar Quaternary deposits (e.g. Steinen et al., 1987; Leslie et al., 1992; Koban and Schweigert, 1993; Evans, 1999; Melezhik and Fallick, 2001). The study of ancient travertines and tufas remains a challenge, however, especially when they are only partly exposed at the surface.

We describe a Paleocene travertine system, presently only partly exposed, in the Itaboraí basin (Fig. 1), a small half-graben in the state of Rio de Janeiro, southeastern Brazil. The travertine was preserved because it was quickly buried by Paleocene–Eocene alluvial fans in a subsiding basin. Due to its high purity, the travertine was mined to exhaustion for cement in half a century (1933–1984), leaving only an artificial lake in the central part of the basin. Before mining ceased, several authors described the macroscopic appearance, geometry, and fossil content of the travertine in quarry exposures and outcrops in the basin and discussed its genesis (e.g. Leinz, 1938; Rodrigues-Francisco and Cunha, 1978). Currently, a few outcrops are still exposed along the borders of the basin, and core samples from several boreholes drilled during mining activity are available. We integrate field and core data with petrographic (LTr, SEM/EDS, and CL) and geochemical (isotopic and elemental compositions) analyses of the carbonate lithofacies, which together bear directly on the origin of the paleotravertine system and the source of the travertine-depositing waters. In addition, we discuss the influence of abiotic and biotic processes on the carbonate precipitation, according to petrographic and geochemical data.

2. Geological setting

The Itaboraí basin, located 34 km NE of the city of Rio de Janeiro (Figs. 1 and 2), is a small half-graben, 1.5 km long and 0.5 km wide, in the eastern part of the continental rift of southeastern Brazil (CRSB) (Riccomini, 1989; Riccomini et al., 1996). The rift, of Cenozoic age, is an ENE-trending, narrow, elongate trough, approximately 1000 km long, that stretches from Curitiba (Paraná) in the WSW to Barra de São João (Rio de Janeiro) in the ENE (Fig. 1). The Itaboraí basin (also called the São José de Itaboraí basin in prior research) records the earliest (Paleocene) stage in the formation of the CRSB as a result of late processes related to the break up of Gondwana, the separation of Brazil from Africa, and the opening of the south Atlantic Ocean. In the early Tertiary, NNW–SSE regional extension related to thermomechanic tilting of the adjoining offshore Santos basin reactivated ENE shear zones within the Precambrian basement, which led to the generation of continental half-grabens (Riccomini 1989). The Itaboraí basin formed along an ENE-trending normal fault (Riccomini and Rodrigues-Francisco, 1992) that limited its southern border and served as the conduit for rising waters (Rodrigues-Francisco and Cunha, 1978).

The carbonate rocks of the Itaboraí basin were attributed to a travertine system by Leinz (1938), who first described these deposits. His assumption was based on the irregular, lenticular geometry, textural features, and high purity of

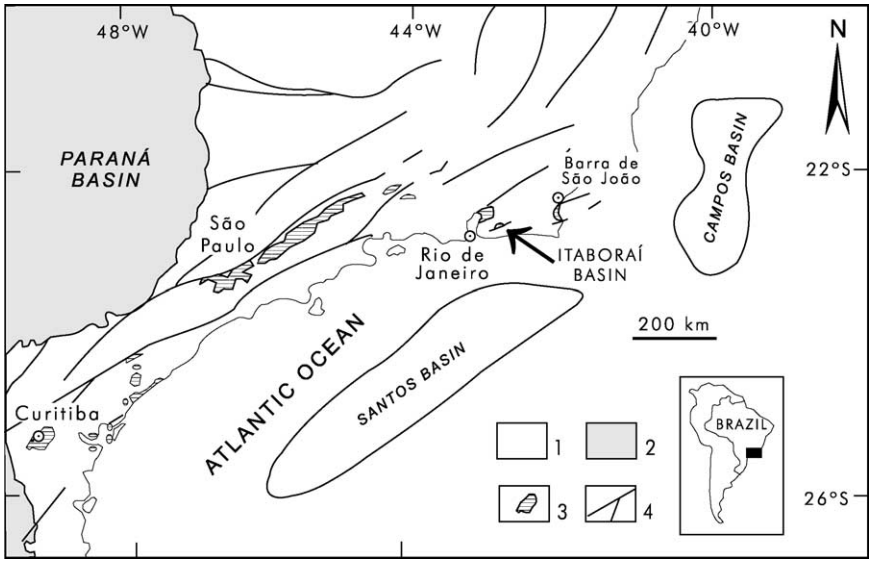

Fig. 1. Regional context of the continental rift of southeastern Brazil (CRSB) (modified from Riccomini et al., 1996) and location of the Itaboraí basin. (1) Precambrian basement; (2) Paleozoic and Mesozoic sedimentary and volcanic rocks of the Paraná basin; (3) Tertiary sedimentary deposits of the CRSB; and (4) Precambrian shear zones, partially reactivated in the Mesozoic and Cenozoic.

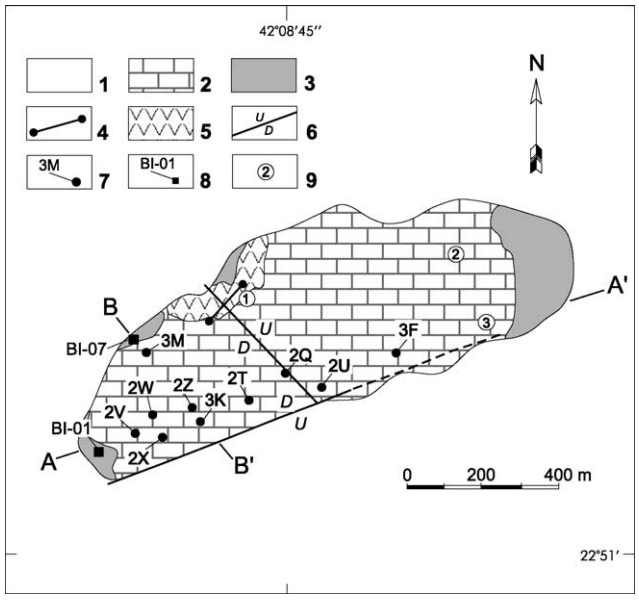

Fig. 2. Geological map of the Itaboraí basin (modified from Rodrigues-Francisco and Cunha, 1978). (1) Basement rocks; (2) travertine deposits; (3) alluvial deposits; (4) ankaramite dike; (5) inferred extent of the ankaramite lavas; (6) fault (dashed where covered) (U, upthrown block; D, downthrown block); (7) borehole locations; (8) sampled outcrops; and (9) karstic features (dissolution channels). A–A′, B–B′ are cross-sections in Figs. 3 and 4, respectively.

the calcareous layers. Precambrian marbles, detected only in the subsurface of gneissic country rocks, were postulated as the source of Ca-rich, travertine-depositing waters (Rodrigues-Francisco and Cunha, 1978). A NW–SE-trending, predominantly normal fault separated the basin into two parts, with the downthrown block to the WSW (Fig. 2). As a result, carbonate layers in this block dip SSE up to 30°, whereas in the ENE block, bedding remains subhorizontal.

The carbonate rocks comprise several facies, such as banded travertine and grey limestone (Leinz, 1938), pisoid layers (Menezes and Curvello, 1973; Tibana et al., 1984), arborescent travertine, and tufa (Tibana et al., 1984). The calcareous sequence is thickest in the southwestern part of the basin and thins toward the north and east (Rodrigues-Francisco and Cunha, 1978).

At the eastern and northern borders, the travertine deposits exhibit karstic features, mainly dissolution channels (Fig. 2). The channels were filled with marls and collapse breccias that contained a wide variety of terrestrial fossils, including Tertiary gastropods (Maury, 1935; Mezzalira, 1946; Ferreira and Coelho, 1971; Palma and Brito, 1974), seeds (Magalhães, 1950; Beurlen and Sommer, 1954), and a very important primitive fossil mammal fauna (orders Condylarthra, Notoungulata, Litopterna, Astrapotheria, Xenungulata, and Marsupialia) of late Early–early Late Paleocene age (Bergqvist and Ribeiro, 1998). Marshall (1985) previously attributed this vertebrate fauna to the middle Late Paleocene. Fossil mammals and terrestrial gastropods also are preserved in travertines outside the dissolution channels. Leaves (Magalhães, 1948), fungal spores (Curvello, 1981), and fossil wood (Rodrigues-Francisco, 1975; Mussa et al., 1987) also have been found in the basin.

Siliciclastic rocks (mudstones, sandstones, and conglomerates) derived from gneissic source areas around the basin were deposited by subaerial mudflows in an alluvial fan system (Tibana et al., 1984; Sant'Anna, 1999) and interfinger with and overlie the carbonate sequence with sharp contacts. The palynological analysis of a coal-bearing horizon (lignite) interlayered with alluvial fan deposits at the northern border of the basin yields a Paleocene–Eocene age, as indicated by the key species *Foveotriletes margaritae*, *Echitricolpites polaris*, and *Verrutriporites lunduensis* (Lima and Cunha, 1986). Nodular pedogenic calcretes also are present in the alluvial fan deposits exposed at the eastern border of the basin (Tibana et al., 1984; Sant'Anna et al., 2000).

An ankaramitic lava flow interlayered with conglomerates of the alluvial fan system at the northern border of the basin (Klein and Valença, 1984) has been dated as Early–Middle Eocene (52.6 ± 2.4 Ma, K/Ar age) by Riccomini and Rodrigues-Francisco (1992).

3. Sample locations

Ten cores were employed in this study. The travertine samples were taken from nine of these cores, ranging in length from approximately 9 to 120 m: eight come from close to the southern border (cores 2V, 2W, 2X, 2Z, 3K, 2T, 2Q and 3F), and one (core 3M) comes from the northwestern border of the basin (Fig. 2). The set of studied cores (Figs. 3 and 4) displays the entire carbonate section (81.3 m maximum thickness) in the Itaboraí basin, including its contacts with both basement gneisses and marbles and the overlying alluvial fan deposits. Carbonate facies change laterally within a few meters, making lateral lithological correlation among the cores impossible. In addition, samples of a tufa deposit were collected from an outcrop at the western border of the basin (BI-01, Fig. 2).

Core 2U (50.3 m in length) from near the intersection of faults that trend NW–SE and ENE contains only basement rocks (Fig. 3). Basement rocks also were recovered from two other cores close to the southern border of the basin. In the cores, the marble is usually unweathered and occurs as decimetric- to metric-scale lenses within gneisses, which in turn are weathered.

4. Methods

Samples were sorted first by standard hand-specimen techniques to recognize carbonate facies. Uncovered polished thin sections of representative samples of the diverse facies subsequently were prepared and examined with a conventional petrographic microscope (LTr).

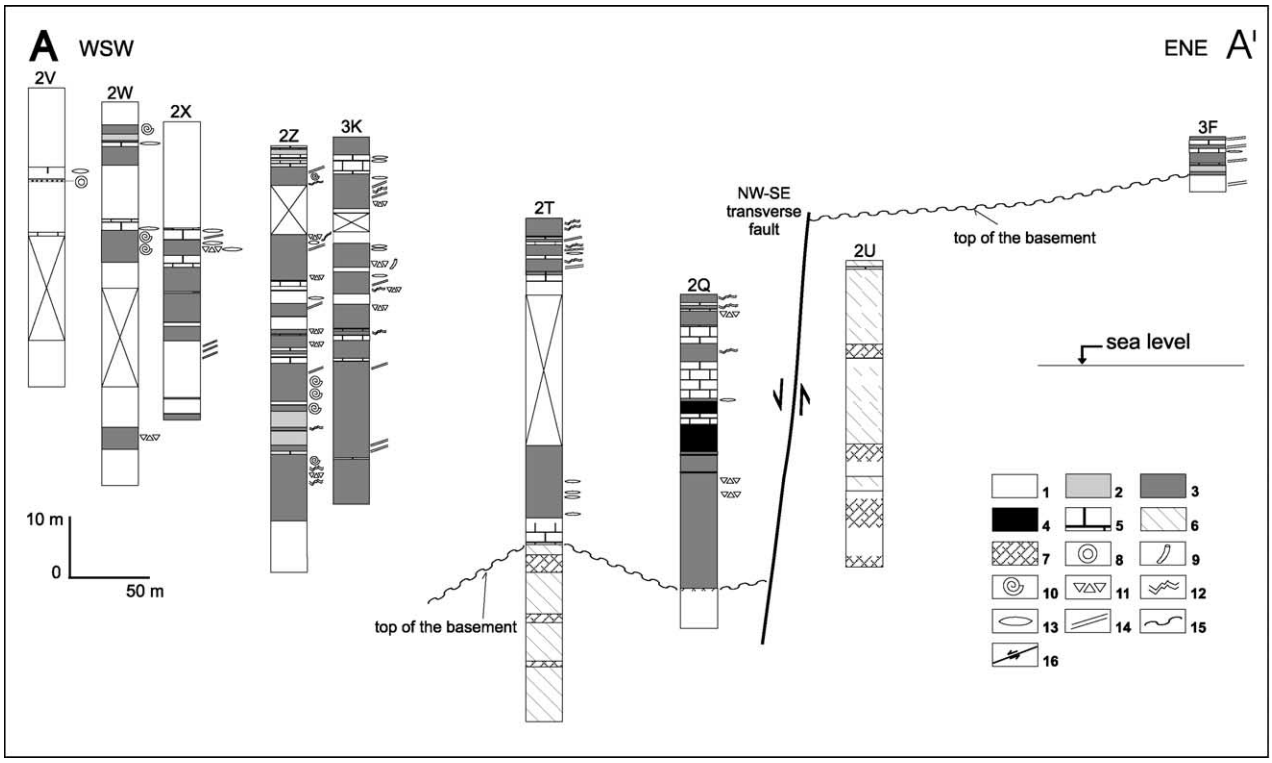

Fig. 3. Stratigraphic section of the cores along A–A′ (see Fig. 2). (1) Mudstone, sandstone, and conglomerate of alluvial fans; (2) lithoclast travertine; (3) micritic travertine; (4) black pure micritic travertine; (5) crystalline crust travertine; (6) gneiss; (7) marble; (8) pisoids; (9) burrows; (10) gastropods; (11) breccia; (12) irregular desiccation fractures; (13) vugs; (14) travertine-filled tectonic fractures; (15) unconformity; and (16) fault.

The same thin sections were observed under cathodoluminescence (CL) on a Luminoscope MkII (12 kV, 250 μA) to identify zonation and diagenetic alterations.

Microtextural studies, including observation of crystalline habits, were carried out on small fragments and thin sections coated with a thin layer of carbon in JEOL JSM-T330A and LEO-440i scanning electron microscopes (SEM), both coupled with energy dispersive spectrometers (EDS). The search for bacterial forms under the SEM followed the method described by Folk and Lynch (1997), in which samples are etched with 1% HCl for 1 min and coated with gold for 20 s.

X-ray diffraction (XRD) was employed to confirm the carbonate mineralogy and identify the silicate minerals in impure travertines and tufas. The XRD analyses were performed on whole-rock samples and their respective acid-resistant (dilute HCl) residues in a Siemens D5000 X-ray diffractometer equipped with Göbbel mirrors and that uses Cu Kα radiation.

Elemental Sr was determined in selected whole rocks by inductively coupled plasma-mass spectrometry (ICP-MS). These analyses were done at Activation Laboratories Ltd (Actlabs), Canada, where the samples were dissolved by the fusion method. The Sr isotope composition of selected travertine samples was determined in the Isotope Geology Laboratory of the Federal University of Pará (Pará-Iso).

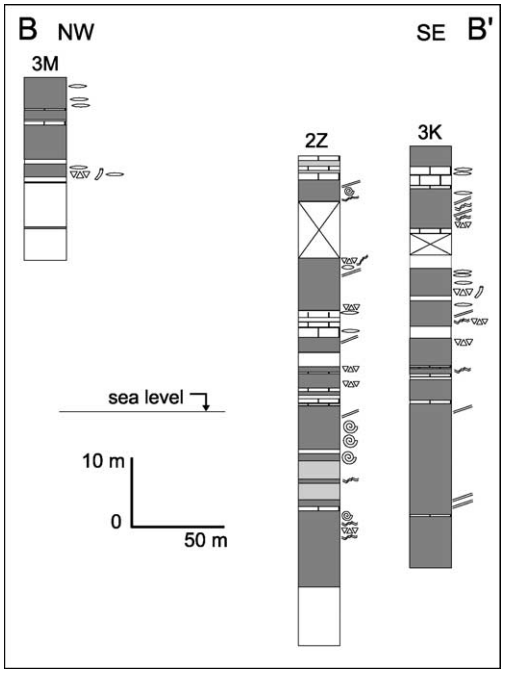

Fig. 4. Stratigraphic section of cores along B–B′ (see Fig. 2). See Figure 3 for symbols.

Sample preparation for Sr isotopic analysis involved the dissolution of 4–5 mg of powdered sample with 2.0 N triple-distilled HCl. Sr was separated from the matrix using EiChrom SrSpec resin, following standard chromatographic techniques. Strontium isotope ratios were measured on a Finnigan-MAT 262 multicollector thermal ionization mass spectrometer using statical modes. The NBS (SRM) 987 standard was analyzed with the samples, and a $^{87}Sr/^{86}Sr$ mean value of 0.710223 ± 13 (2σ) was obtained. Analytical errors are quoted in 2σ.

Carbon and oxygen isotopic analyses were performed for selected samples (10–15 mg weight) drilled from polished rock slabs and carried out at the Stable Isotope Laboratory (LABISE) of the Department of Geology, Federal University of Pernambuco (UFPE). CO_2 gas was extracted from powdered samples in a high vacuum line after reaction with 100% phosphoric acid at 25 °C for one day. The CO_2 released, after cryogenic cleaning, was analyzed in a double inlet, triple-collector SIRA-II mass spectrometer; the results are reported in δ notation, PDB scale, in permil (‰). The BSC (Borborema skarn calcite) reference gas that was calibrated against NBS-18, NBS-19, and NBS-20 standards was used ($\delta^{18}O = -11.28$‰ PDB and $\delta^{13}C = -8.58$‰ PDB). The precision of the method has been assessed by repeated analyses of the BSC reference gas and the accuracy by comparison with NBS standards ($\delta^{18}O = -2.12$‰ PDB and $\delta^{13}C = +1.89$‰ PDB was found for NBS-19). The uncertainties of the isotope measurements were 0.1‰ for carbon and 0.2‰ for oxygen.

5. Carbonate lithofacies in the Itaboraí basin

Carbonate lithofacies include travertines and tufa. Travertine types are as follows: (1) crystalline crusts, (2) pisoids, (3) micrites, and (4) lithoclasts. Among the rock types mentioned by previous authors, only arborescent travertine, described in the central part of the basin as composed of fibrous-radiating calcite (Tibana et al., 1984), was not recovered.

5.1. Crystalline crust travertine

The crystalline crust travertine exhibits the most representative macroscopic and microscopic features of the travertine system in the Itaboraí basin. It appears as irregular and lenticular beds up to tens of meters in length and several meters in thickness (Leinz, 1938) and mainly occurs close to the ENE-trending fault at the southwestern border of the basin, west of the NW–SE transverse fault (Fig. 2). Crystalline crusts also occur as veins that fill subhorizontal to vertical tectonic fractures (up to tens of centimeters wide) with regular, planar walls that cut basement rocks (marbles and gneisses in cores 2U and 3F at the southern border), alluvial deposits (outcrop BI-07), and other travertines (impure and pure micritic travertines in several cores) (see Fig. 2). Ferrari (2001) describes travertine-filled veins, centimeters to decimeters wide and several meters long, cutting the Precambrian basement along the SW segment of the ENE fault.

Crystalline crusts are non-fossiliferous, dense, layered, and generally white. The layers are composed of coarse to extremely coarse crystalline calcite fibers (more than 0.1 mm to several centimeters long) that are essentially perpendicular to the depositional surfaces and form dense aggregates. Under LTr, the crystals exhibit fibrous to bladed habit with subhedral to euhedral terminations and subparallel to feathery orientation (Fig. 5A and B). The CL reveals a zoned pattern in the fibrous calcite, marked by alternating submillimetric luminescent (orange) and dully luminescent (dark brown) zones (Fig. 5C). Rare millimetric to centimetric layers containing more equant calcite crystals may be interlayered with fibrous calcite layers (Fig. 5D). The equant calcite is non-luminescent and coarse to very coarse (0.2–1.3 mm). None of these white calcareous layers produces any residue after treatment with HCl, and whole-rock analyses by XRD show only calcite in their composition.

The crystalline crusts alternate with brown ferruginous layers, which gives rise to a submillimetric to centimetric banding defined by planar to wavy laminae (Fig. 5E). After treatment, ferruginous laminae covering fibrous calcite (Fig. 5F–H) are revealed as composed of radiating aggregates of parallel lath-like crystal bundles (mostly <2 μm in length) of goethite (Fig. 5I). Hexagonal crystal forms (probably basal sections of calcite), but no bacterial or nanobacterial forms such as those described in many recent papers (e.g. Folk and Lynch, 1997; Chafetz and Guidry, 1999), were observed, even under high magnification (100,000×).

5.2. Pisoid travertine

Pisoid travertines occur in small, irregular lenses (several centimeters thick and tens of centimeters long), commonly within the crystalline crusts along the major ENE axis of the basin (Menezes and Curvello, 1973; Tibana et al., 1984). Medeiros and Bergqvist (1999) also describe oolitic banks and marls with ooids and pisoids. Presently, pisoid travertines are not exposed but were recovered from core 2V (Figs. 2 and 3).

Samples of pisoid-bearing lenses exhibit graded structure, with small pisoids (1–2 mm) grading to coarser ones (3–5 mm). Gradation toward the periphery of pisoid lenses deposited near the ENE fault has been observed by Medeiros and Bergqvist (1999). In general, the pisoids appear to float in the cement, but in some places, adjacent pisoids exhibit point contacts. Individual pisoids are smooth and spheroidal and less commonly exhibit elongate or geometric shapes inherited from their nuclei (Fig. 6A). Terrigenous detrital grains, fragments of broken pisoids, or calcite crystals ordinarily constitute their nuclei. The pisoids are concentrically laminated and banded (alternating light

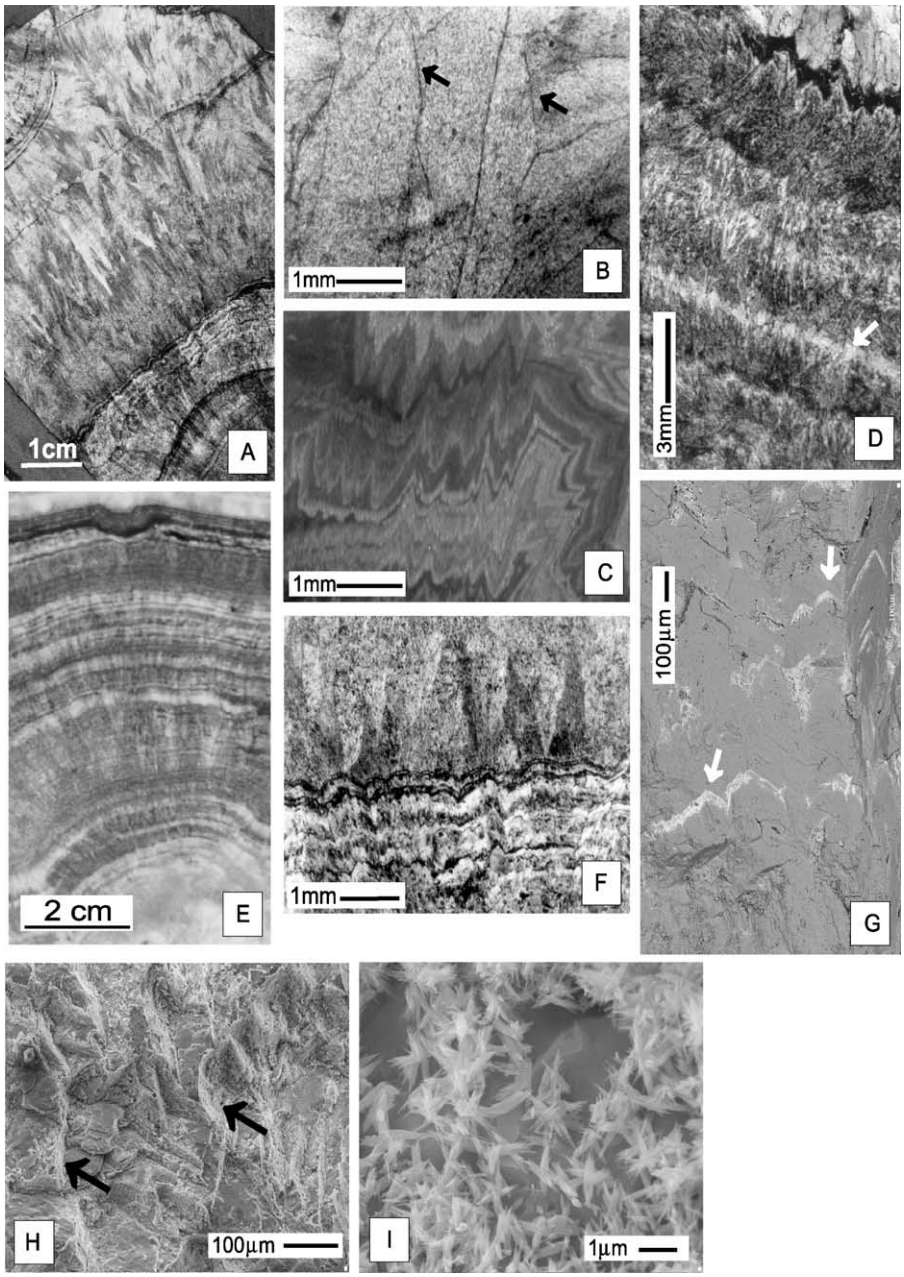

Fig. 5. Textures and fabrics of the crystalline crust travertine. (A) Photomicrograph of thin section showing fan-like to feathery fibrous calcite. (B) Photomicrograph of thin section showing detail of the fibrous calcite with well-developed crystal faces (arrows). (C) CL image of zoned fibrous calcite (same area as B). (D) Photomicrograph of thin section illustrating alternating bands of fibrous and more equant calcite (arrow). (E) Hand sample showing white and brown banding of the crystalline crust travertine. (F) Photomicrograph of thin section detailing the brown ferruginous laminae alternated with white fibrous calcite. (G) SEM image of discontinuous (arrows) ferruginous layers located at the terminations of fibrous calcite crystals (BSE image). (H) SEM image of thin ferruginous layers coating calcite crystals (arrows). (I) SEM image of aggregates of the goethite crystals from ferruginous layers.

yellow and brown layers), are a few micra wide, and have well-defined boundaries according to both LTr and SEM (Fig. 6B and C). The light layers are composed of dully luminescent, very finely crystalline (5–10 μm) equant calcite crystals (Fig. 6B and D), and the brown layers contain luminescent (orange) cryptocrystalline (<3 μm) calcite (Fig. 6B and D). The EDS data obtained for calcite of very finely crystalline and cryptocrystalline layers show iron in the spectra of the coarser crystals (5–10 μm) (Fig. 6E and F), consistent with their dull luminescence, and only Ca in the smaller crystals (<3 μm) (Fig. 6G and H).

5.3. Micritic travertine

Micritic travertines make up irregular beds (centimeters to several meters wide; Leinz, 1938) and probably are the most widespread lithofacies in the Itaboraí basin, where

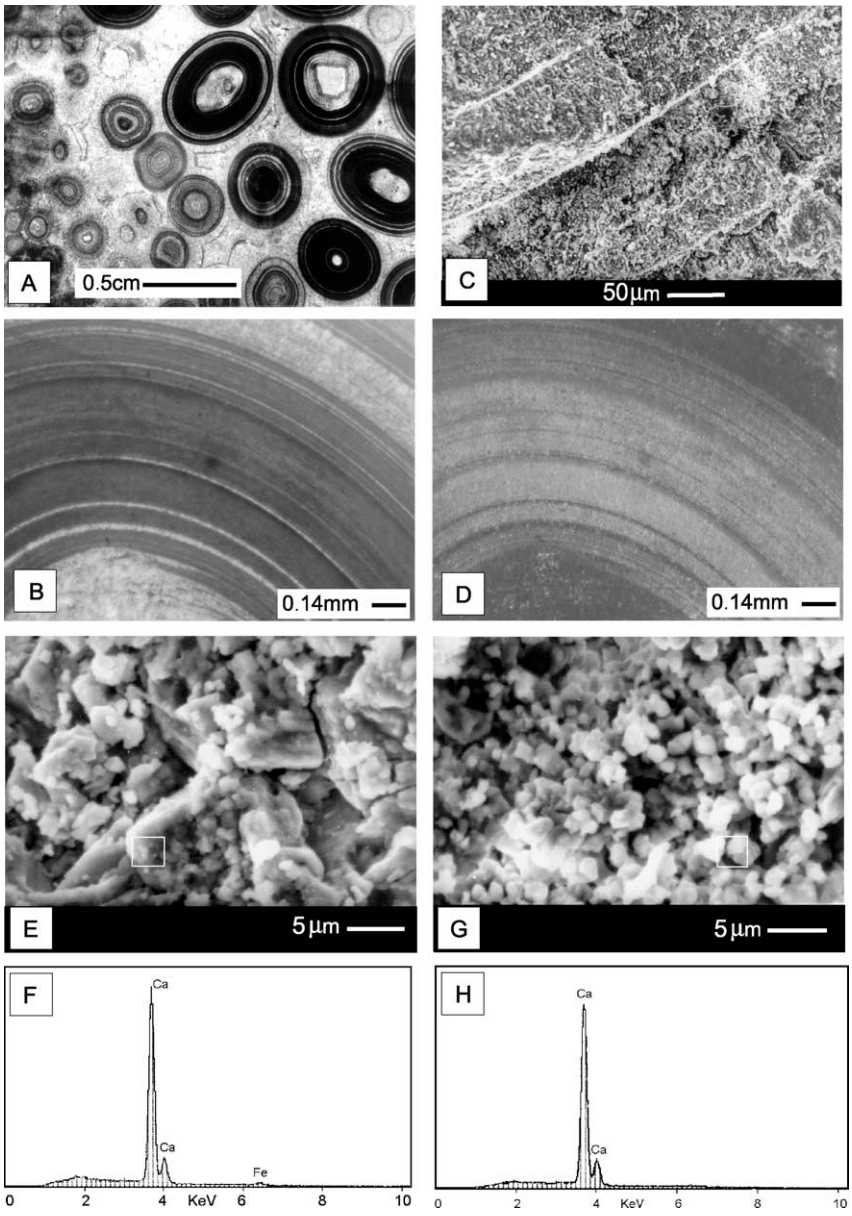

Fig. 6. Textures and fabrics of pisoid travertine. (A) Graded spherical pisoids containing angular nuclei and interpisoid cement. (B) Photomicrograph of the well-defined, even laminae of the pisoids. (C) SEM image of the fine crystalline and cryptocrystalline layers of the pisoid. (D) CL image of the same area as in B. (E) SEM image of the coarser calcite. (F) EDS spectrum from the white square in E, revealing the presence of iron. (G) SEM image of the finer calcite. (H) EDS spectrum from the white square in G showing Ca only.

they occur interbedded with other travertine, as well as with the alluvial fan deposits. The micritic travertines are massive and comprise a very fine crystalline to cryptocrystalline (<10 µm in diameter) calcite matrix with up to 40% angular detrital grains. Limestones with less than 2% terrigenous sand and silt (mostly quartz and feldspar) are considered pure micritic travertines and generally are beige in color and weakly luminescent (brownish-orange). A particular restricted lithofacies is a dark-colored (dark brown to black), pure micritic travertine, found only in the middle part of core 2Q (Figs. 2 and 3) near the NW–SE fault at the southern border of the basin. This travertine contains fine iron sulfide (pyrite) disseminated in the matrix (Fig. 7A–C).

Impure micritic travertines (2–40% siliciclastic particles) are usually light colored (beige, light grey to light green) and contain silt- to pebble-graded detrital grains (quartz, feldspar, mica, and lithic fragments), well-preserved terrestrial gastropods, and the clay minerals kaolinite and smectite, according to XRD analyses of insoluble residues. Both pure and impure micritic travertines contain angular reworked intraclasts of themselves and crystalline crusts. Circumgranular cracking and microfractures, which represent desiccation cracks, are common in the pure micritic

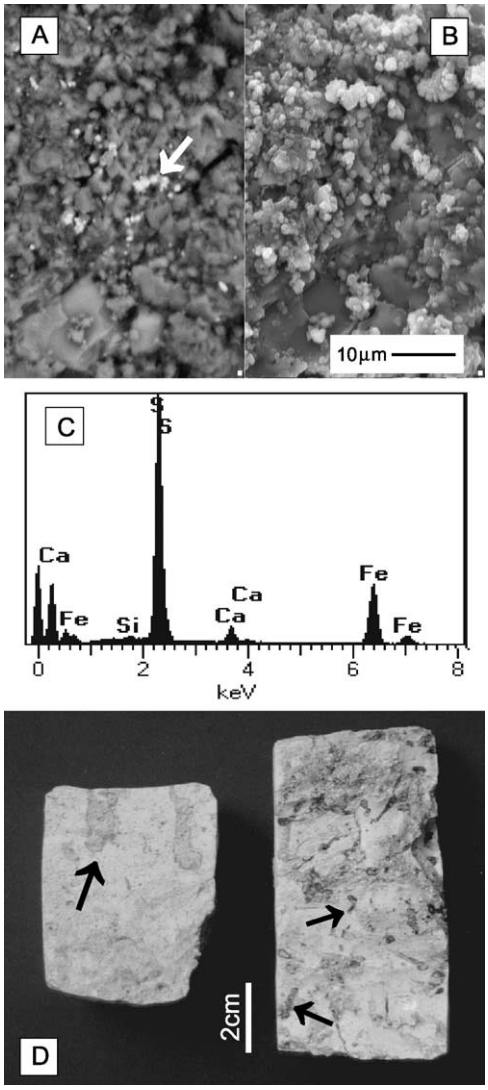

Fig. 7. Aspects of the fabric of the micritic travertine. (A) SEM image (BSE) showing fine iron sulfide crystals (pyrite; see arrow) disseminated in the matrix. (B) SE image of the same area as in A. (C) EDS spectrum of iron sulfide. (D) Bioturbation features (arrows) in borehole samples of pure micritic travertine.

travertines. Macroscopic bioturbation features (mudstone-filled burrows) are widespread in some layers of this lithofacies (Fig. 7D).

5.4. Lithoclast travertine

Beige to brown, porous, friable lithoclast travertine is one of the scarcest lithofacies in the Itaboraí basin; it occurs only in cores 2Z and 3F (Figs. 2 and 3). It is made up of sand-sized fragments of crystalline crust and micritic travertines weakly cemented by calcite.

5.5. Tufa

Fossiliferous porous tufa with calcareous rhizoliths were described in the central part of the basin (Tibana et al., 1984) and remain exposed at its western border (Fig. 8A). Rhizoliths, comprising rhizocretions and root casts (in the sense of Mount and Cohen, 1984), occur as straight tubes 3–5 mm in diameter and 2–5 cm long (Fig. 8B). They are vertically oriented in a very finely crystalline to cryptocrystalline calcite matrix with minor amounts of detrital grains (mica, quartz) and terrestrial gastropods (Fig. 8C). Root sheaths are brownish and composed of non-luminescent fibrous calcite (Fig. 8D and E). Root casts consist of mudstone or dully luminescent calcite. No relict organic root materials were found.

6. Geochemistry

We present the geochemical data, including carbon and oxygen isotopes, elemental Sr, and $^{87}Sr/^{86}Sr$ ratios, in Table 1. We also plot the $\delta^{13}C$ and $\delta^{18}O$ isotopic results in Fig. 9.

6.1. Carbon and oxygen analyses

The white layers of the crystalline crust travertines yield $\delta^{18}O$ values ranging from −12.1 to −5.4‰ PDB and $\delta^{13}C$ values between −5.3 and −0.4‰ PDB (Table 1, Fig. 9). The brown crystalline crusts have $\delta^{18}O$ between −9.0 and −5.5‰ PDB and $\delta^{13}C$ between −5.7 and −0.9‰ PDB. Light-colored and black pure micritic travertines show $\delta^{18}O$ values ranging from −9.6 to −6.0‰ PDB and $\delta^{13}C$ from −3.4 to 0.0‰ PDB. The impure micritic travertines have negative values of $\delta^{18}O$ (−7.8 to −6.5‰ PDB) and $\delta^{13}C$ (−2.0 to −0.8‰ PDB). Stable isotopic data obtained for a root sheath correspond to $\delta^{18}O = -9.1$‰ PDB and $\delta^{13}C = -3.6$‰ PDB; for a whole pisoid, the values are $\delta^{18}O = -6.4$‰ PDB and $\delta^{13}C = -2.1$‰ PDB. Fracture-filling crystalline crusts have $\delta^{18}O$ values between −11.9 and −5.8‰ PDB and $\delta^{13}C$ between −7.3 and −1.1‰ PDB.

6.2. Strontium analyses

The Sr content measured in white crystalline crust travertines displays a wide range: 275–1170 ppm (Table 1). For the same lithofacies, the $^{87}Sr/^{86}Sr$ ratios vary between 0.710973 and 0.713398. $^{87}Sr/^{86}Sr$ is 0.712174 for one sample of fracture-filling crystalline crust. Precambrian marbles yield $^{87}Sr/^{86}Sr$ ranging 0.706208–0.706443 (Table 1).

7. Discussion

7.1. Origin and depositional settings of the paleotravertine system

The reactivation of the ENE shear zone in the Precambrian basement by the early Tertiary NNW–SSE

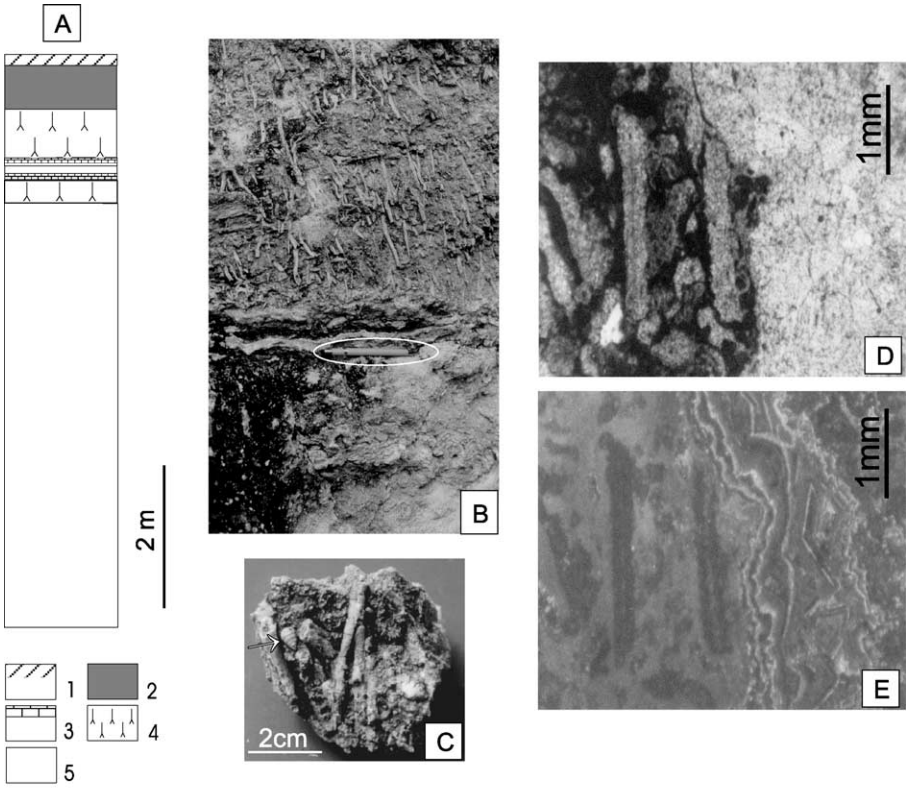

Fig. 8. (A) Columnar section of a tufa deposit at outcrop BI-01 (see Fig. 2): (1) soil; (2) micritic travertine; (3) crystalline crust travertine; (4) tufa; and (5) alluvial fan deposits. (B) General view of the tufa with abundant calcareous rhizoliths. Pencil (in flattened ellipse) for scale. (C) Rhizoliths and terrestrial gastropod (arrow) in the tufa. (D) Photomicrograph of thin section of vertically oriented rhizoliths (left side of the photo) in matrix. (E) CL image of area in D showing the non-luminescent calcite of the root sheath and matrix (left) and the zoned luminescent pattern of the second calcite cement (right).

extensional event promoted the installation of the hemi-graben and the generation of the travertine system of the Itaboraí basin. Synsedimentary tectonic activity controlled basin subsidence, as is indicated by the increasing thickness of the travertines against the ENE fault surface, as well as by the presence of crystalline crusts as tectonic vein fillings that cut basement rocks, travertines, and alluvial fan deposits. Spring-related travertine and active tectonics is a highly expected association, especially in a rift basin controlled by normal faulting. Faults and vein fractures form the main conduits for a large volume of fluids (Sibson, 1996), and travertines usually accumulate close to (within 1–2 km) normal faults and can be used to trace them (Hancock et al., 1999). The importance of the ENE fault to the generation of the travertine system in the Itaboraí basin already has been noted by previous authors (Leinz, 1938; Rodrigues-Francisco and Cunha, 1978; Medeiros and Bergqvist, 1999), who also recognize its role as the main conduit for the spring waters at the southern border of the basin—an ancient site of subsidence where the crystalline crust travertine is abundant.

The absence of a lateral correlation of travertine layers between cores is a common facies attribute in travertine systems developed around springs, because of the rapid carbonate precipitation, irregular topography of the terrain, and changes in spring location. We have interpreted the depositional settings of the carbonate lithofacies in accordance with petrographic data, facies associations in the cores, and the geometry of the layers as described by previous authors (Leinz, 1938; Rodrigues-Francisco and Cunha, 1978). In the Itaboraí basin, the depositional settings apparently were highly variable, according to the lithofacies variability in the cores.

The crystalline crusts of Itaboraí basin display putatively primary macroscopic and microscopic fabrics (see Braithwaite, 1979; Leslie et al., 1992; Kendal and Iannace, 2001), very similar to those described in ray crystal crusts (Folk et al., 1985; Chafetz and Guidry, 1999). This fabric is very distinctive in travertine deposits formed around springs (e.g. Guo and Riding, 1992, 1998), where fibrous to bladed calcite with subparallel to feathery orientation precipitates from agitated, rapidly flowing water (Folk et al., 1985; González et al., 1992; Guo and Riding, 1992, 1998). The fast fluid flow, usually present in irregular surfaces (slope, spring orifice, pool edge), constantly supplies the growing crystals with reactants (González et al., 1992) and causes the rapid loss of CO_2 (Folk et al., 1985). Similar conditions may have occurred at the southwestern border of the basin, close

Table 1
Carbon and oxygen isotopes, Sr content, and $^{87}Sr/^{86}Sr$ ratios of the travertines of the Itaboraí basin

Lithofacies	Sample	$\delta^{18}O_{PDB}$ (‰)	$\delta^{13}C_{PDB}$ (‰)	Sr (ppm)	$^{87}Sr/^{86}Sr$
White crystalline crust	2Q	−8.0	−0.4		
White crystalline crust	2QD	−11.7	−2.1	1170	0.710973
White crystalline crust	2T	−12.1	−1.6	460	0.713398
White crystalline crust	2ZG-BR	−5.4	−5.3		
White crystalline crust	2ZN-BR	−11.2	−0.8	896	0.711489
White crystalline crust	3KA	−8.6	−3.1	275	
White crystalline crust	3MI-BR	−6.8	−4.2		
White crystalline crust	3MJ-BR	−9.0	−0.7		
White crystalline crust	3MK-BR	−11.6	−1.6	1010	0.711421
White crystalline crust	SJ3F-A7	−11.0	−2.1		0.712174
Brown crystalline crust	2ZG-MR	−6.5	−4.0		
Brown crystalline crust	2ZN-MR	−9.0	−1.3		
Brown crystalline crust	3MJ-MR	−8.0	−1.3		
Brown crystalline crust	3MK-MR	−6.2	−5.4		
Brown crystalline crust	SJ2Z1	−6.3	−2.7		
Brown crystalline crust	SJ2Z4F	−7.6	−5.7		
Brown crystalline crust	SJ2T1	−5.5	−1.1		
Brown crystalline crust	SJ2T2	−7.5	−0.9		
Brown crystalline crust	SJ3FA	−5.7	−4.5		
Brown crystalline crust	SJ3FC	−6.6	−1.4		
Brown crystalline crust	SJ3FD	−6.0	−2.4		
Brown crystalline crust	IT-1C	−7.0	−2.2		
Beige pure micritic travertine	2TF	−7.0	0.0	808	
Beige pure micritic travertine	2ZC	−6.8	−2.4	2310	
Beige pure micritic travertine	3KE	−8.2	−1.1	689	
Beige pure micritic travertine	3M-L	−6.6	−2.0		
Beige pure micritic travertine	SJ2Z3	−6.0	−3.4		
Beige pure micritic travertine	SJ2Z4M	−6.8	−1.8		
Beige pure micritic travertine	SJ2Z5	−7.2	−0.7		
Beige pure micritic travertine	SJ3K1	−6.8	+0.1		
Black pure micritic travertine	SJ2Q2	−9.6	−1.2		
Black pure micritic travertine	SJ2Q10	−8.8	−0.2		
Impure micritic travertine	3M-M	−7.8	−2.0		
Impure micritic travertine	SJ3MA	−7.2	−0.8		
Impure micritic travertine	SJ3MB	−6.5	−1.4		
Impure micritic travertine	IT-1A	−7.5	−2.0	327	
Pisoid	2VH	−6.4	−2.1		
Root	IT-1B	−9.1	−3.6		
Fracture-filling crystalline crust	3FB	−11.9	−1.9		0.711539
Fracture-filling crystalline crust	IT7A-1A	−7.2	−2.3		
Fracture-filling crystalline crust	IT7A-2A	−7.1	−1.9		
Fracture-filling crystalline crust	IT7A-3A	−5.8	−5.1		
Fracture-filling crystalline crust	IT7A-5A	−6.5	−5.5		
Fracture-filling crystalline crust	IT7A-6A	−11.0	−1.1		
Fracture-filling crystalline crust	IT7B-2B	−9.6	−1.6		
Fracture-filling crystalline crust	IT7B-3B	−8.8	−7.3		
Fracture-filling crystalline crust	IT7B-5B	−5.9	−5.7		
Fracture-filling crystalline crust	IT7B-6B	−10.5	−1.2		
Marble	2TEMB1				0.706208
Marble	2TEMB3				0.706245
Marble	2UE				0.706443

to the ENE normal fault, where irregular layers of crystalline crusts are abundant and constitute the most representative lithofacies of the travertine system.

The lenses of pisoid travertine are interpreted as representative of deposition in small pools (see Guo and Riding, 1998, Fig. 3, p. 167) near the springs, as is suggested by their close association with the crystalline crusts. The concentrically laminated structure of the pisoids is indicative of their generation under turbulent water flux (Folk and Chafetz, 1983; Guo and Riding, 1998).

Carbonate mud is the most common lake-fill travertine facies (Chafetz and Folk, 1984; Pentecost and Viles, 1994). The fast-flowing waters around the springs at the southwestern border of the basin eventually reached its central and lateral portions and formed small, shallow ponds in which micritic travertine precipitated. Detrital grains

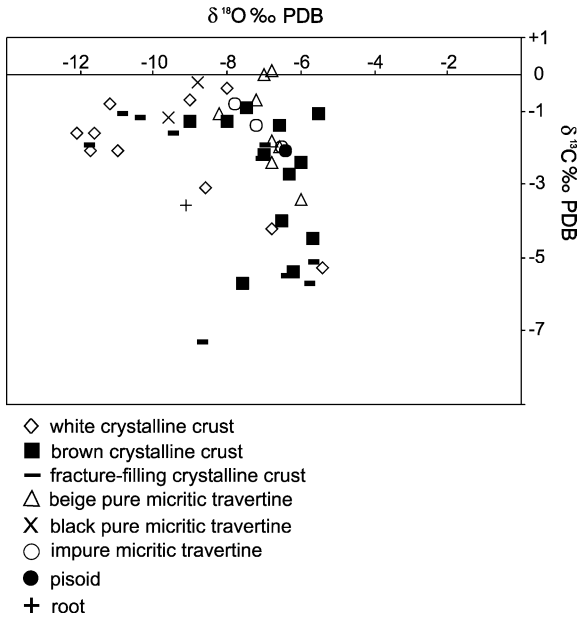

Fig. 9. C and O isotopic data for travertines and tufa from the Itaboraí basin.

and terrestrial fossils (gastropods and mammal remains) from the surrounding countryside may have been wasted into the basin, across the alluvial fans, and deposited in the ponds, where they generated impure micritic travertines.

The erosion of travertines and the deposition of lithoclastic material in depressions in the basin (e.g. Guo and Riding, 1998) gave rise to the lithoclast travertine. In the basin, the erosion of crystalline crusts and micritic travertines may have furnished angular fragments to flat areas, where they were weakly cemented by calcite to form lithoclast travertine.

At the borders of the basin, far from the springs, conditions were favorable for tufa deposition. The presence of rhizoliths suggests the encrustation of macrophytes in pools, probably as paludal tufas (Evans, 1999). Root sheaths probably formed around living and decaying roots. Detrital grains and terrestrial gastropods were transported into the tufa pools by distal alluvial fans.

The surficial deposition of the carbonate lithofacies in the Itaboraí basin allowed for bioturbation and subaerial alteration in the micritic travertines, which led to desiccation-generated brecciation and the disruption of fabrics, as well as the formation of calcretes in the alluvial fans. These features indicate intermittent subaerial exposure and pedogenesis of the sediments during deposition. The lithoclast travertines at the southern border of the basin and the intraclasts observed in the micritic travertines also indicate surficial reworking of previously deposited sediments.

7.2. Source of the carbonate waters—Sr analyses

Since Beurlen and Sommer's (1954) study, the source of the Ca-rich spring waters has been attributed to the dissolution of Precambrian marble in the basement of the Itaboraí basin. $^{87}Sr/^{86}Sr$ ratios for white fibrous calcite of the crystalline crusts range from 0.711 to 0.713, which is higher than the mean ratio (0.706) for the Precambrian marble (Table 1). This enrichment in radiogenic ^{87}Sr in the travertines indicates that the marble was not the only source of strontium in the groundwaters. The Precambrian marble occurs as lenses within gneisses, for which $^{87}Sr/^{86}Sr$ ratios are not available, but their age and silicate composition are appropriate for the input of ^{87}Sr into the percolating groundwaters. The contribution of marble is recorded, however, by $^{87}Sr/^{86}Sr$ ratios that are lower than would be expected for silicate-derived strontium in a purely gneissic terrain (0.715–0.722) (Faure and Powell, 1972; Faure, 1986). The strontium in the Itaboraí basin therefore represents a mixture of these two sources. Strontium in solution could be generated in marble and gneiss aquifers or perhaps developed within rocks originally fractured and faulted in Precambrian ENE shear zones and then subjected to further brittle deformation in the early Cenozoic. The marble is not exposed at the surface and probably is volumetrically less important than the gneisses in the basement. Nevertheless, its imprint in the groundwater isotopic composition is expected, considering that recognition of carbonate-derived strontium is possible even in drainage basins that contain only 5–10% carbonate rocks (Fisher and Stueber, 1976).

Additional evidence of the mixed source of the carbonate waters is the wide range of values for the Sr content of the white fibrous calcite of the crystalline crusts (275–1170 ppm) (Table 1). These values (mainly 800–1000 ppm) are consistent with those reported for travertines from central Italy (Barbieri et al., 1979), where the depositing waters interacted with marine limestones and evaporites.

7.3. The influence of abiotic and biotic processes

The Itaboraí crystalline crust travertine is composed of fibrous calcite that exhibits a sharply zoned pattern (with dull and orange luminescent layers) and goethitic laminae alternated with the calcitic layers. No bacterial forms were observed in the calcitic crusts, in agreement with the general observation that fibrous calcite precipitates by abiotic processes (Chafetz and Guidry, 1999). However, several authors have suggested that ferruginous micritic laminae interfingered with crystalline crusts indicates biogenic influence (e.g. Leslie et al., 1992). Moreover, Casanova et al. (1999) describe microbially mediated ferrihydrite from modern carbonate travertines. Thus, though no bacterial forms were found in the ferruginous layers composed of goethite, biotic mediation of iron oxide precipitation cannot be excluded.

The zoned pattern of fibrous calcite indicates periodic change in the composition of the carbonate-precipitating water, which is commonly recorded in modern travertine

springs (e.g. Kitano, 1963). Visible CL in sedimentary carbonates can be explained by a concentration of coprecipitated minor elements, mainly Mn as an activator and Fe as a quencher of CL (Marshall, 1988). Budd et al. (2000) recognize that Mn is the sole control on CL intensity in carbonates with very low concentrations (<100 ppm) of Mn and Fe. A minimum of 25 ppm Mn is necessary to activate visible CL in calcite cements. In the Itaboraí basin, zonation in the fibrous calcite thus appears to be due to variations in Mn concentration, not iron. The lack of interference by iron, despite its availability in the environment, may be explained by the independent precipitation of iron oxide and calcite, as described by Kitano (1963), who observed calcium carbonate precipitating at the water–atmosphere interface and $Fe_2O_3 \cdot nH_2O$ precipitating separately in the water column in active hot springs. Alternatively, geomorphology may have controlled iron oxide and carbonate precipitation, as recognized by Casanova et al. (1999) in an active travertine deposit, where the oxide forms before the carbonate in flat areas and simultaneously on sloping substrates. Chafetz et al. (1998) relate the sequence of precipitation of Fe-oxides, Mn-oxides and carbonates to increases in pH and Eh in the water flowing from the spring. They also recognize a bacterial influence in concentrating Mn and Fe in shrub-like precipitates. According to Schwertmann and Fisher (1973), ferrihydrite evolves to a crystalline form within a few hours after precipitation in the absence of impurities. If this occurred in the Itaboraí travertine, bacterial cells have not been preserved to prove it.

In conclusion, Mn and Fe probably were carried together by the spring waters flowing along the ENE fault at the south border of the Itaboraí basin, but at the surface, these elements were precipitated separately, one substituting for calcium in the calcite (originating the CL-zoned pattern) and the other as an iron oxide deposited over the calcite crystals. The influence of physical (topography of the depositional areas), chemical (pH and Eh), and biological (biotically induced oxide and/or carbonate precipitation) factors, acting together or independently, is highly probable.

The pisoid travertines exhibit evidence of an inorganic origin, such as their spherical shape and concentrically laminated structures. Such characteristics previously have been interpreted as evidence of formation in strongly agitated waters and control by inorganic chemical precipitation (Folk and Chafetz, 1983).

Some biotic influence almost certainly existed in the precipitation of micritic travertines in shallow waters. For example, the presence of fine pyrite disseminated in the micritic matrix of black pure micritic travertine suggests the activity of sulphate-reducing bacteria in the depositional environment.

The role played by macro- and micro-organisms in the genesis and lithification of tufa deposits has been recognized (e.g. Viles and Goudie, 1990). The cementation of living and decaying roots to form rhizoliths in tufa (Klappa, 1980) is probably, if not certainly, a biotically mediated process.

7.4. Stable isotopes

Fig. 9 shows the relatively large variations in the stable isotopic composition of the travertines precipitated in the Itaboraí basin. The white crystalline crusts exhibit the largest spread of $\delta^{13}C$ and $\delta^{18}O$ values, varying by 5 and 7‰, respectively. A comparable scale is recorded by the fracture-filling crystalline crusts. These variations probably reflect changes in the chemistry of the waters at the time of deposition, in agreement with the interpretation based on the CL-zoned pattern of the fibrous calcite. A variable isotopic composition is frequently recorded in modern travertines and might be related to changes in the water composition in the spring outlets and/or its flux downstream (Turi, 1986; Amundson and Kelly, 1987; Chafetz and Lawrence, 1994).

In addition, considerable overlap among the values of distinct travertine types is observed (Fig. 9). Pure and impure micritic travertines, crystalline crusts containing ferruginous material, a pisoid, and a root sheath from the tufa deposit all display the same range in $\delta^{18}O$ and $\delta^{13}C$ compositions. This overlap among travertines from different depositional settings might indicate that other factors, in addition to the chemistry of the water, influenced carbonate precipitation at each site. In general, the isotopic composition of the water changes downflow and acquires progressively higher ^{13}C and ^{18}O concentrations as the system reequilibrates and the CO_2 escape decreases with distance from the spring (Gonfiantini et al., 1968; Friedman, 1970). In the Itaboraí basin, the $\delta^{13}C$ and $\delta^{18}O$ values seem to be products of the interaction between the original isotopic composition of the formation water and several factors related to surficial conditions and precipitation, such as location of the material with respect to the spring and changes in the rate and/or mechanism of precipitation (abiotic versus biotic) (Usdowski et al., 1979; Chafetz and Lawrence, 1994). The nature of our study, which is devoted to a fossil occurrence and lacks data about the formation water and original environmental conditions, hampers any evaluation of the relative importance of each factor in controlling the travertine isotope composition.

8. Conclusions

Study of the Itaboraí basin represents a unique opportunity to compare information from outcrops and borehole cores on Paleocene travertine and tufa deposits. Because these carbonates have been mined to exhaustion, the interpretations presented here necessarily rely on descriptions of quarry faces and outcrops that were written prior to the cessation of mining. Our descriptions are limited with regard to the geometry and facies relationships of the sedimentary strata because of the nature of travertine systems and the current emphasis on the analysis of core materials. However, the study of fresh travertine samples from boreholes enables us to characterize several previously

unknown microscopic features in the Itaboraí basin. Sampling and geochemical analyses of travertines and basement rocks also are essential for identifying the source of the carbonate-rich waters and show that marble in the basement is not necessarily the only source of calcium and bicarbonate in the spring waters, as previously was believed.

In the Itaboraí basin, travertine generation was the result of a combination of Cenozoic reactivation of an old tectonic structure in the basement and groundwater hydrology. The ENE fault at the southern border of the basin was reactivated by early Tertiary NNW–SSE extension and served as the main conduit for spring waters. The chemical constituents of the groundwater were derived largely from Precambrian basement rocks, including marbles and gneisses. Crystalline crust travertines were deposited mainly around springs. They contain CL-zoned fibrous calcite precipitated inorganically from water that changed in composition in the spring orifice and/or downflow, as is indicated by its stable isotopic composition. Goethitic micritic laminae alternate with white fibrous calcitic layers and give rise to a macroscopic wavy banding. Manganese and iron also were carried to the surface by spring waters; the Mn was incorporated into the calcite, and Fe precipitated as iron oxide. Pisoid travertines formed inorganically in small, turbulent pools, whereas micritic travertines formed distally from the springs in shallow ponds, where they were subject to bioturbation and desiccation. Locally, pyrite precipitated, probably through biotic mediation. Detrital grains and fossil remains were carried by an alluvial fan drainage system into the basin and deposited in the micritic travertines. Tufa also formed distally from the springs, at times encrusting living plants, probably under a biogenic influence. Travertine deposits that formed far from springs probably were influenced by several variables (chemistry of the water, rate and mechanism of precipitation) in their generation. The travertine and tufa deposits are intercalated with and overlain by Paleocene–Eocene alluvial fan deposits, which protected them against erosion.

Acknowledgements

This work was funded by the Fundação de Amparo à Pesquisa do Estado de São Paulo (FAPESP, 95/3381-5, 96/0029-1, 97/12091-6). Important comments and suggestions were given by Lluis Cabrera (Universidad de Barcelona, Spain) during fieldwork in 1996 and 1998. The authors thank Thomas Rich Fairchild (University of São Paulo, Brazil) for improving the English of a first version of the text, Fernando Pellon de Miranda for providing research facilities at the Petróleo Brasileiro S/A (Petrobrás), and André Luiz Ferrari (Universidade Federal Fluminense, Brazil) for discussions and guidance in the field. Thanks are also due to Victor de Carvalho Klein (Universidade Federal do Rio de Janeiro, Brazil) and Joel Carneiro de Castro (Universidade Estadual Paulista, Rio Claro, Brazil) for information about the Itaboraí basin. The authors are also grateful to reviewers Dilce de Fátima Rossetti and Francesco Dramis and the regional editor, Reinhardt Fuck, whose suggestions improved the manuscript.

References

Altunel, E., Hancock, P.L., 1993. Morphology and structural setting of Quaternary travertines at Pamukkale, Turkey. Geological Journal 28, 335–346.

Altunel, E., Hancock, P.L., 1994. Active fissuring and faulting in Quaternary travertines at Pamukkale, western Turkey. Zeitschrift fur Geomorphologie-Supplement band 94, 285–302.

Amundson, R., Kelly, E., 1987. The chemistry and mineralogy of a CO_2-rich travertine depositing spring in the California Coast Range. Geochimica et Cosmochimica Acta 51, 2883–2890.

Barbieri, M., Masi, U., Tolomeo, L., 1979. Origin and distribution of strontium in the travertines of Latium (Central Italy). Chemical Geology 24, 181–188.

Bergqvist, L.P., Ribeiro, A.M., 1998. A paleomastofauna das bacias eoterciárias brasileiras e sua importância na datação das bacias de Itaboraí e Taubaté, In: Paleógeno de América del Sur y de la Península Antártica, Publicación Especial 5. Associación Paleontológica Argentina, Buenos Aires, Argentina pp. 19–34.

Beurlen, K., Sommer, F.W. Restos vegetais fósseis e tectônica da Bacia Calcárea de Itaboraí, Estado do Rio de Janeiro. Boletim do Departamento Nacional de Produção Mineral, Divisão de Geologia e Mineralogia 149. 27 pp

Braithwaite, C.J.R., 1979. Crystal textures of Recent fluvial pisolites and laminated crystalline crusts in Dyfed, South Wales. Journal of Sedimentary Petrology 49, 181–194.

Budd, D.A., Hammes, U., Ward, W.B., 2000. Cathodoluminescence in calcite cements: new insights on Pb and Zn sensitizing, Mn activation, and Fe quenching at low trace-element concentrations. Journal of Sedimentary Research 70, 217–226.

Casanova, J., Bodénan, F., Négrel, P., Azaroual, M., 1999. Microbial control on the precipitation of modern ferrihydrite and carbonate deposits from the Cézallier hydrothermal springs (Massif Central France). Sedimentary Geology 126, 125–145.

Chafetz, H.S., Folk, R.L., 1984. Travertines: depositional morphology and the bacterially constructed constituents. Journal of Sedimentary Petrology 54, 289–316.

Chafetz, H.S., Guidry, S., 1999. Bacterial shrubs, crystal shrubs, and ray-crystal shrubs: bacterial vs. abiotic precipitation. Sedimentary Geology 126, 57–74.

Chafetz, H.S., Lawrence, R., 1994. Stable isotopic variability within modern travertines. Géographie physique et Quaternaire 48, 257–273.

Chafetz, H.S., Akdim, B., Julia, R., Reid, A., 1998. Mn- and Fe-rich black travertine shrubs: bacterially and nanobacterially induced precipitates. Journal of Sedimentary Research—Section A: Sedimentary Petrology and Process 68, 404–412.

Curvello, W.S., 1981. Esporos de fungos na bacia cálcaria S. José, Itaboraí, RJ. Anais da Academia Brasileira de Ciências 54, 754.

Evans, J.E., 1999. Recognition and implications of Eocene tufas and travertines in the Chadron Formation, White River Group, Badlands of South Dakota. Sedimentology 46, 771–789.

Faure, G., 1986. Principles of Isotope Geology. Wiley, New York.

Faure, G., Powell, J.L., 1972. Strontium Isotope Geology. Springer, Heidelberg.

Ferrari, A.L., 2001. Evolução tectônica do Graben da Guanabara. PhD Thesis. University of São Paulo, Brazil, 412 pp.

Ferreira, C.S., Coelho, A.C.S., 1971. Novos gastrópodes pulmonados da Bacia Calcária de São José de Itaboraí, RJ, Brasil. Geocronologia. Anais da Academia Brasileira de Ciências 43 (Supplemento), 463–472.

Fisher, R.S., Stueber, A.M., 1976. Strontium isotopes in selected streams within the Susquehanna river basin. Water Resources Research 12, 1061–1068.

Folk, R.L., Chafetz, H.S., 1983. Pisoliths (pisoids) in Quaternary travertines of Tivoli, Italy, in: Peryt, T.M. (Ed.), Coated Grains. Springer, Berlin, pp. 474–487.

Folk, R.L., Lynch, F.L., 1997. Nannobacteria are alive on Earth as well as Mars, Proceedings Reprint, Instruments, Methods, and Missions for the Investigation of Extraterrestrial Microorganisms, vol. 3111. The International Society for Optical Engineering, San Diego, CA, pp. 406–419.

Folk, R.L., Chafetz, H.S., Tiezzi, P.A., 1985. Bizarre forms of depositional calcite in hot-spring travertines, central Italy, in: Schneidermann, N., Harris, P.M. (Eds.), Carbonate cements Society of Economic Paleontologists and Mineralogists Special Publication 36, pp. 349–369.

Ford, T.D., Pedley, H.M., 1996. A review of tufa and travertine deposits of the world. Earth-Science Reviews 41, 117–175.

Fouke, B.W., Farmer, J.D., Des Marais, D.J., Pratt, L., Sturchio, N.C., Burns, P.C., Discipulo, M.K., 2000. Depositional facies and aqueous-solid geochemistry of travertine-depositing hot springs (Angel Terrace, Mammoth Hot Springs, Yellowstone National Park, USA). Journal of Sedimentary Research 70, 565–585.

Friedman, I., 1970. Some investigations of the deposition of travertine from hot springs: I. The isotopic chemistry of a travertine-depositing spring. Geochimica et Cosmochimica Acta 34, 1303–1315.

Gonfiantini, R., Panichi, C., Tongiorgi, E., 1968. Isotopic disequilibrium in travertine deposition. Earth and Planetary Science Letters 5, 55–58.

González, L.A., Carpenter, S.J., Lohmann, K.C., 1992. Inorganic calcite morphology: roles of fluid chemistry and fluid flow. Journal of Sedimentary Petrology 62, 382–399.

Guo, L., Riding, R., 1992. Aragonite laminae in hot water travertine crusts, Rapolano Terme, Italy. Sedimentology 39, 1067–1079.

Guo, L., Riding, R., 1998. Hot-spring travertine facies and sequences, Late Pleistocene, Rapolano Terme, Italy. Sedimentology 45, 163–180.

Hancock, P.L., Chalmers, R.M.L., Altunel, E., Çakir, Z., 1999. Travitonics: using travertines in active fault studies. Journal of Structural Geology 21, 903–916.

Kendall, A.C., Iannace, A., 2001. 'Sediment'–cement relationships in a Pleistocene speleothem from Italy: a possible analogue for 'replace-replacement' cements and *Archaeolithoporella* in ancient reefs. Sedimentology 48, 681–698.

Kitano, Y., 1963. Geochemistry of calcareous deposits found in hot springs. Journal of Earth Sciences of the Nagoya University 2, 68–100.

Klappa, C.F., 1980. Rhizoliths in terrestrial carbonates: classification, recognition, genesis and significance. Sedimentology 27, 613–629.

Klein, V.C., Valença, J.G., 1984. Estruturas almofadadas em derrame ankaramítico na Bacia de São José de Itaboraí, Rio de Janeiro. Anais do 33° Congresso Brasileiro de Geologia. Sociedade Brasileira de Geologia, Rio de Janeiro, Brazil 9, 4335–4345.

Koban, C.G., Schweigert, G., 1993. Microbial origin of travertine fabrics—two examples from southern Germany (Pleistocene Stuttgart Travertines and Miocene Riedöschingen Travertine). Facies 29, 251–264.

Leinz, V., 1938. Os calcários de São José, Niterói, Estado do Rio. Mineração e Metalurgia 3, 153–155.

Leslie, A.B., Tucker, M., Spiro, B., 1992. A sedimentological and stable isotopic study of travertines and associated sediments within Upper Triassic lacustrine limestones, South Wales, UK. Sedimentology 39, 613–629.

Lima, M.R., Cunha, F.L.S., 1986. Análise palinológica de um nível linhítico da Bacia de São José de Itaboraí, Terciário do Estado do Rio de Janeiro, Brasil. Anais da Academia Brasileira de Ciências 58, 579–588.

Magalhães, J., 1948. Sobre a ocorrência de vegetal fóssil na Fazenda São José, Município de Guaxindiba, RJ. Mineração e Metalurgia 75, 194.

Magalhães, J., 1950. Sobre a ocorrência de *Acrocarpus santosi* sp. nov., no Eocênio Inferior de São José de Itaboraí (Estado do Rio de Janeiro). Revista Científica 1, 42–43.

Marshall, L.G., 1985. Geochronology and land-mammal biochronology of transamerican faunal interchange, in: Stehli, F.G., Webb, S.D. (Eds.), The Great American Interchange. Plenum Press, New York, pp. 50–85.

Marshall, D.J., 1988. Cathodoluminescence of geological materials. Unwin-Hyman, Boston.

Maury, C.J., 1935. New genera and new species of fossil terrestrial mollusca from Brazil. American Museums Novitates 764, 2.

Medeiros, R.A., Bergqvist, L.P., 1999. Paleocene of the São José de Itaboraí Basin, Rio de Janeiro, Brazil: lithostratigraphy and biostratigraphy. Acta Geologica Leopoldensia XXII (48), 3–22.

Melezhik, V.A., Fallick, A.E., 2001. Paleoproterozoic travertines of volcanic affiliation from a ^{13}C-rich rift lake environment. Chemical Geology 173, 293–312.

Menezes, S.O., Curvello, W.S., 1973. Oolititos de Itaboraí, RJ. Anais da Academia Brasileira de Ciências 45, 245–252.

Mezzalira, S., 1946. Australorbis itaboraiensis, n. sp. Revista do Instituto Geográfico e Geológico 4, 158–160.

Mount, J.F., Cohen, A.S., 1984. Petrology and geochemistry of rhizoliths from Plio-Pleistocene fluvial and marginal lacustrine deposits, east Lake Turkana, Kenya. Journal of Sedimentary Petrology 54, 263–275.

Mussa, D., Rodrigues-Francisco, B.H., Cunha, F.L.S., Gonzalez, B.B., 1987. Contribuição à Paleobotânica da Bacia de Itaboraí, RJ. Anais do 1° Simpósio de Geologia RJ-ES. Sociedade Brasileira de Geologia, Rio de Janeiro, Brazil 1987;, 92–101.

Palma, J.M.C., Brito, I.M., 1974. Paleontologia e estratigrafia da Bacia de São José de Itaboraí, Estado do Rio de Janeiro. Anais da Academia Brasileira de Ciências 46, 383–406.

Pentecost, A., 1990. The formation of travertine shrubs: Mammoth Hot Springs, Wyoming. Geological Magazine 127, 159–168.

Pentecost, A., 1991. Springs that turn life into stone. New Scientist 21, 42–44.

Pentecost, A., 1995. The Quaternary travertine deposits of Europe and Asia minor. Quaternary Science Reviews 14, 1005–1028.

Pentecost, A., Tortora, P., 1989. Bagni di Tivoli Lazio: a modern travertine-deposition site and its associated microorganisms. Bollettino della Societá Geologica Italiana 108, 315–324.

Pentecost, A., Viles, H., 1994. A review and reassessment of travertine classification. Géographie Physique et Quaternaire 48, 305–314.

Renaut, R.W., Jones, B., 2000. Microbial precipitates around continental hot springs and geysers, in: Riding, R.E., Awramik, S.M. (Eds.), Microbial Sediments. Springer, Berlin, pp. 187–195.

Riccomini, C., 1989. O Rift Continental do Sudeste do Brasil. PhD Thesis. University of São Paulo, Brazil, 256 pp.

Riccomini, C., Rodrigues-Francisco, B.H., 1992. Idade potássio-argônio do derrame de ankaramito da Bacia de Itaboraí, Rio de Janeiro, Brasil: implicações tectônicas Boletim de resumos do 37° Congresso Brasileiro de Geologia, vol. 2. Sociedade Brasileira de Geologia, São Paulo, Brazil, pp. 469–470.

Riccomini, C., Coimbra, A.M., Sant'Anna, L.G., Brandt Neto, M., Valarelli, J.V., 1996. Argilominerais do paleolago Tremembé e sistemas deposicionais relacionados (Paleógeno, Rift Continental do Sudeste do Brasil). Revista Brasileira de Geociências 26, 167–180.

Rodrigues-Francisco, B.H., 1975. Geologia e estratigrafia da bacia calcárea de São José, Município de Itaboraí, RJ. MSc Dissertation. Institute of Geosciences, Federal University of Rio de Janeiro, Brazil, 89 pp.

Rodrigues-Francisco, B.H., Cunha, F.L.S., 1978. Geologia e estratigrafia da Bacia de São José, Município de Itaboraí, RJ. Anais da Academia Brasileira de Ciências 50, 381–416.

Sanders, J.E., Friedman, G.M., 1967. Origin and occurrence of limestones, in: Chilingar, G.V., Bissel, H.J., Fairbridge, R.W. (Eds.), Carbonate Rocks Developments in Sedimentology, vol. 9A. Elsevier, Amsterdam, pp. 169–265.

Sant'Anna, L.G., 1999. Geologia, mineralogia e gênese das esmectitas dos depósitos paleogênicos do Rift Continental do Sudeste do Brasil. PhD Thesis. University of São Paulo, Brazil, 291 pp.

Sant'Anna, L.G., Riccomini, C., Carvalho, M.D., Sial, A.N., Valarelli, J.V., 2000. Influence of the Geological Setting on the Geochemistry of Pedogenic Calcretes in the Continental Rift of Southeastern Brazil. International Geological Congress, IUGS, Rio de Janeiro, Brazil (CD-Rom Abstracts).

Schwertmann, U., Fisher, W.R., 1973. Natural 'amorphous' ferric hydroxide. Geoderma 10, 237–247.

Sibson, R.H., 1996. Structural permeability of fluid-driven fault-fracture meshes. Journal of Structural Geology 18, 1031–1042.

Steinen, R.P., Gray, N.H., Mooney, J., 1987. A Mesozoic carbonate hot-spring deposit in the Hartford basin of Connecticut. Journal of Sedimentary Petrology 57, 319–326.

Tibana, P., Castro, J.C., Barrocas, S.L.S., 1984. Bacia de Itaboraí. Anais do 33° Congresso Brasileiro de Geologia, Sociedade Brasileira de Geologia, Rio de Janeiro, Brazil 12, 5309–5316.

Turi, B., 1986. Stable isotope geochemistry of travertines, in: Fritz, P., Fontes, J.Ch. (Eds.), Handbook of Environmental Isotope Geochemistry, vol. 2. Elsevier, Amsterdam, pp. 207–238.

Usdowski, E., Hoefs, J., Menschel, G., 1979. Relationship between ^{13}C and ^{18}O fractionation and changes in major element composition in a recent calcite-depositing spring—a model of chemical variations with inorganic $CaCO_3$ precipitation. Earth and Planetary Science Letters 42, 267–276.

Viles, H.A., Goudie, A.S., 1990. Tufas, travertines and allied carbonate deposits. Progress in Physical Geography 14, 19–41.

Waring, G.A., 1965. Thermal springs of the United States and other countries of the world. USGS Professional Paper 492, 383 pp.